# Electronic Supplementary Information

## Photo-chemically assisted redox-nano welding for high conductive and robust copper-based electrodes

Jae-Won Lee,[a] Sang Min Lee,[b] Ji Hye Kwak,[c] Juhee Kim,[d] Sung Jin Kim,[a] Kyong-Soo Hong,[e] Kye Sang Yoo,*[b] Imjeong H.-S Yang,*[a] Hee Jin Jeong,*[d]

[a]*Department of Physics, Pusan National University, Busan 46241, South Korea*

[b] *Department of Chemical & Biomolecular Engineering, Seoul National University of Science & Technology, Seoul 01811, Republic of Korea*

[c]*Electrical Environment Research Center, Power Grid Research Division, Korea Electrotechnology Research Institute (KERI), Changwon 51543, South Korea*

[d]*Nano Hybrid Technology Research Center, Creative and Fundamental Research Division, Korea Electrotechnology Research Institute (KERI), Changwon 51543, Republic of Korea.*

[e]*Busan Center, Korea Basic Science Institute (KBSI), Busan 46742, South Korea*

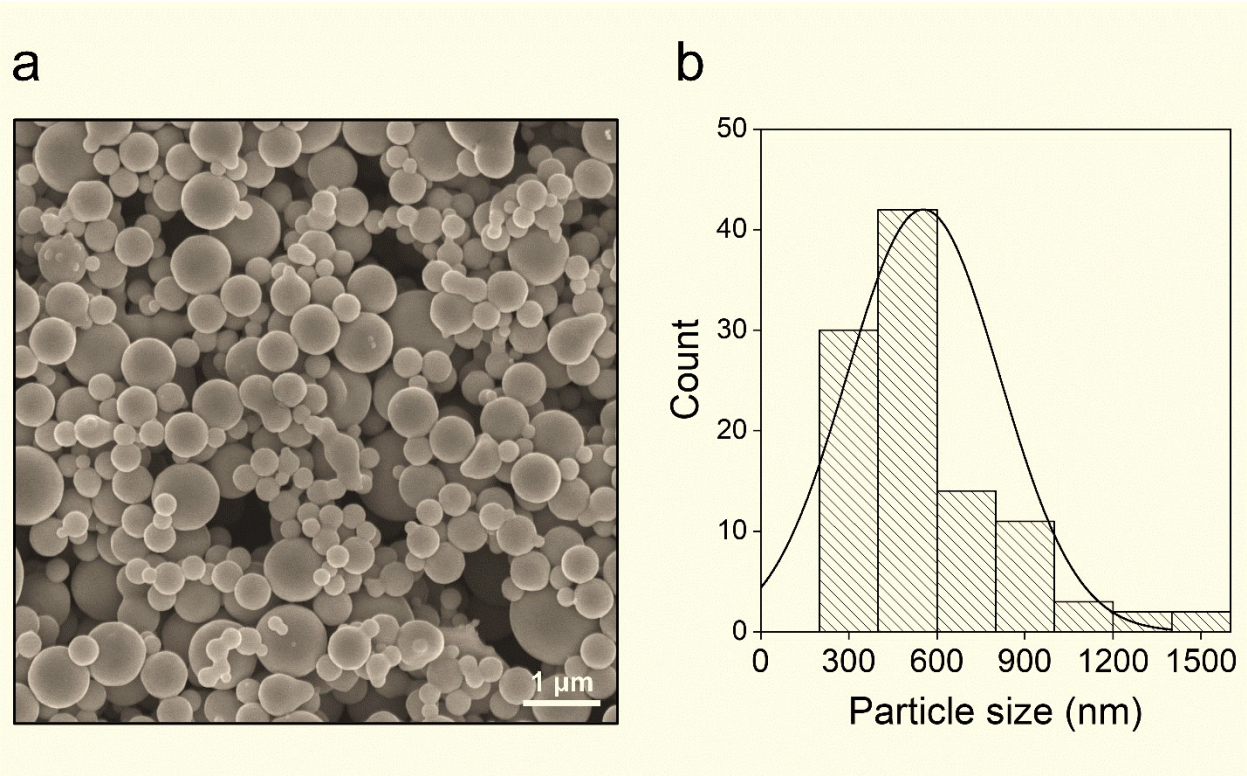


**Fig S1.** (a) SEM image and (b) the corresponding particle size distribution histogram of bare Cu particles

The corresponding normalized particle size distribution histograms shown in Fig. S1b revealed that Cu particles have an average lateral diameter of 551 nm.

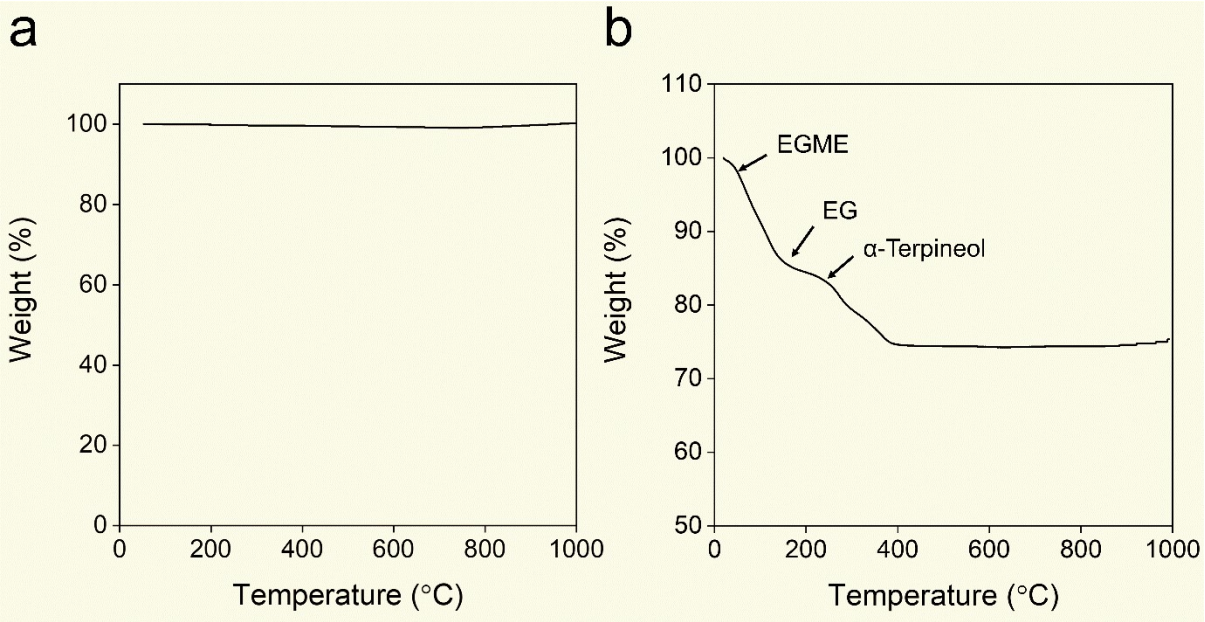


**Fig S2.** TGA results of (a) Cu sub-μPs and (b) Cu sub-μPs based pastes used in this study

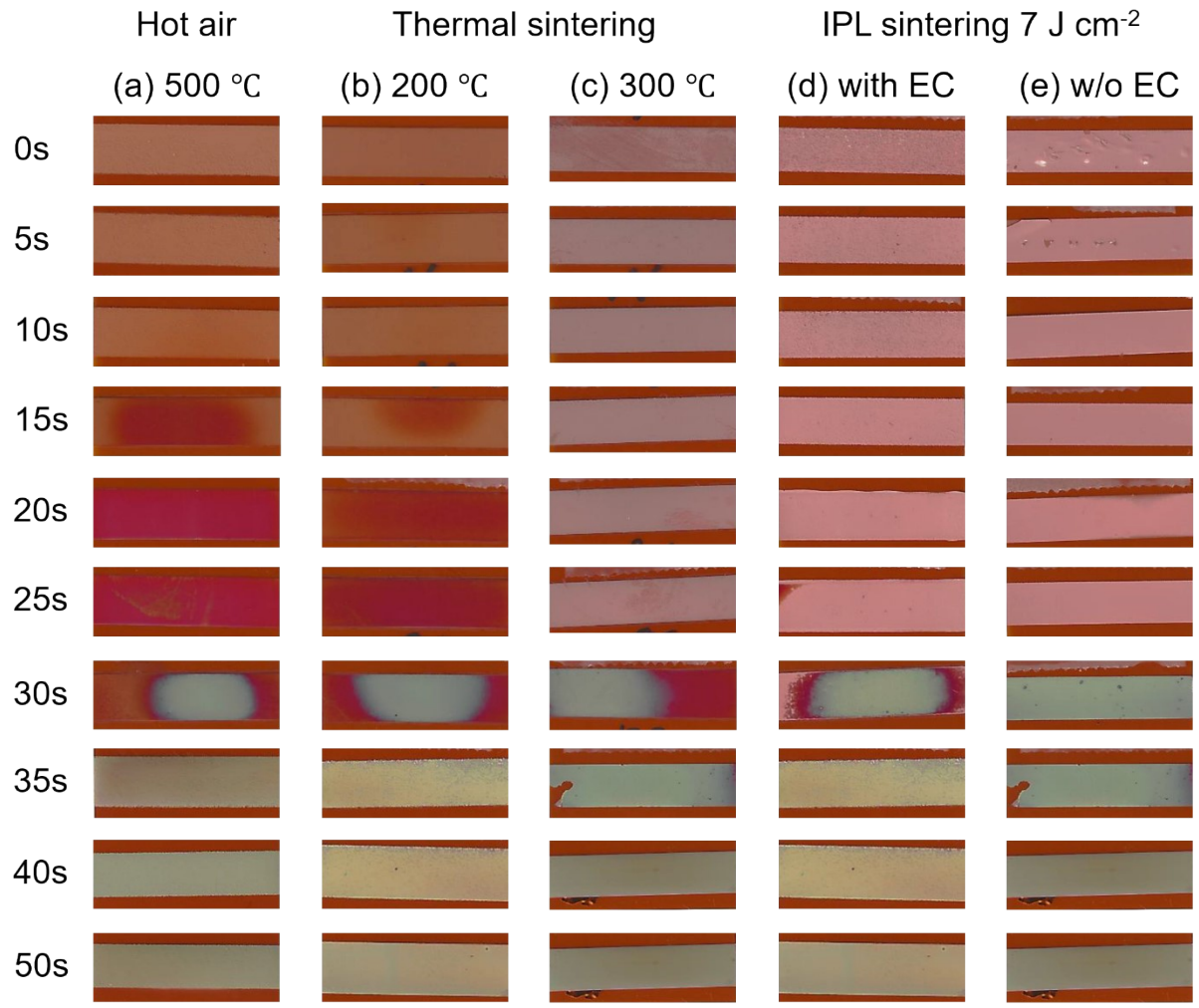


**Fig S3.** Photograph of (a) oxidized Cu sub-μPs electrodes prepared under various oxidation times. Cu sub-μPs electrodes sintered by thermal sintering (b) 200 ℃, (c) 300 ℃. Cu sub-μPs electrodes sintered by IPL irradiation (energy density of 7 J/cm$^2$) (d) with reducing agent, (e) without reducing agent

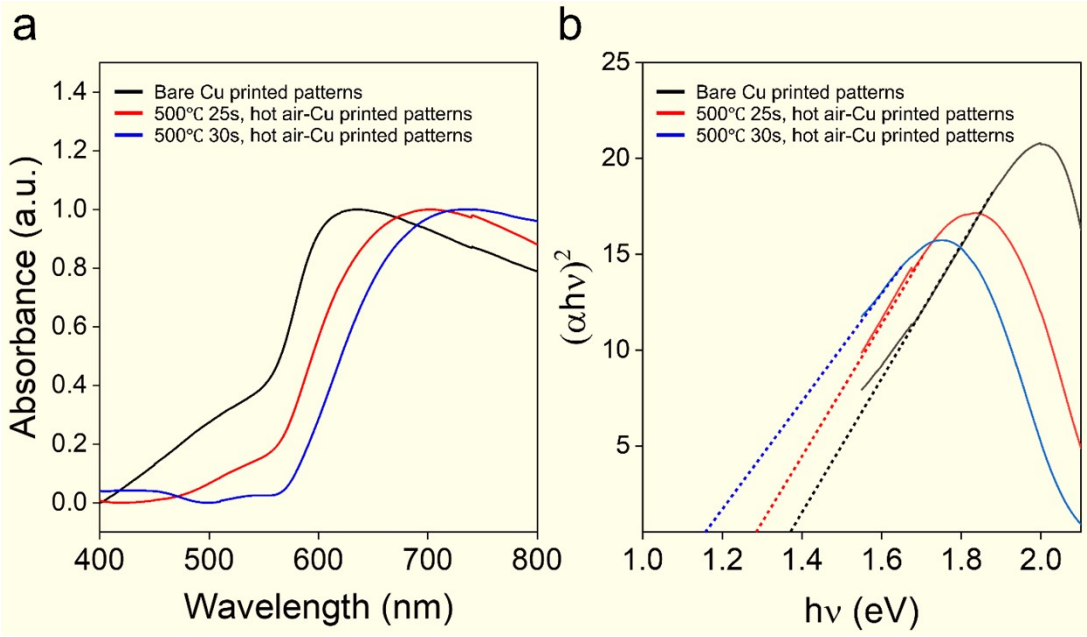


**Fig S4**. (a) Optical properties of bare Cu and oxidized Cu sub-μP patterns (hot air exposure times: 25, 30 s) (a) UV absorption and (b) optical band gap

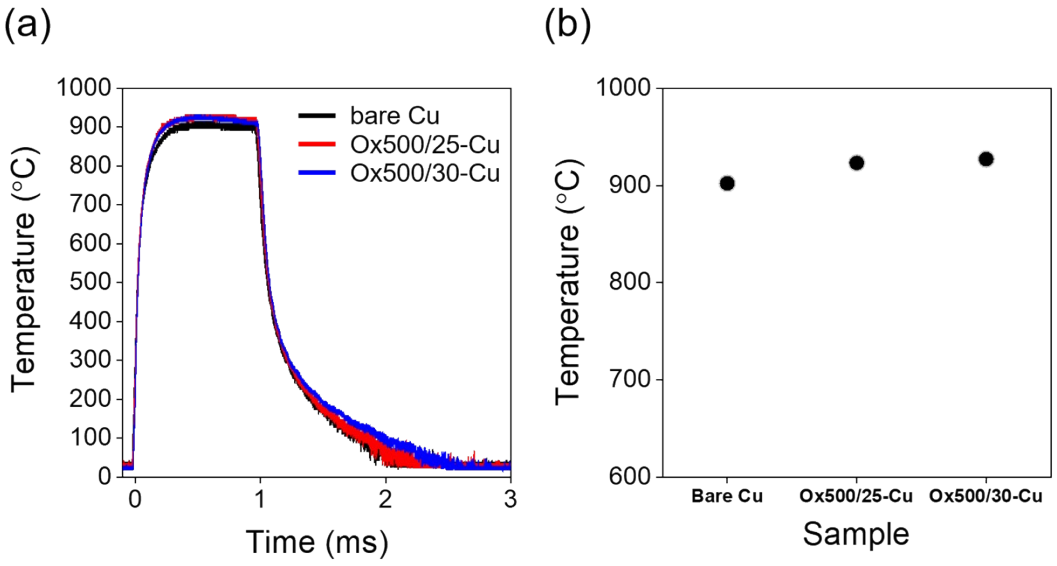


**Fig S5**. (a) Temperature-time profiles of bare Cu and oxidized Cu sub-μP patterns (hot air exposure times: 25, 30 s) during IPL irradiation with a single shot at energy density of 7 J/cm$^2$. (b) Maximum temperatures of bare Cu sub-μP and oxidized Cu sub-μP patterns during IPL irradiation.

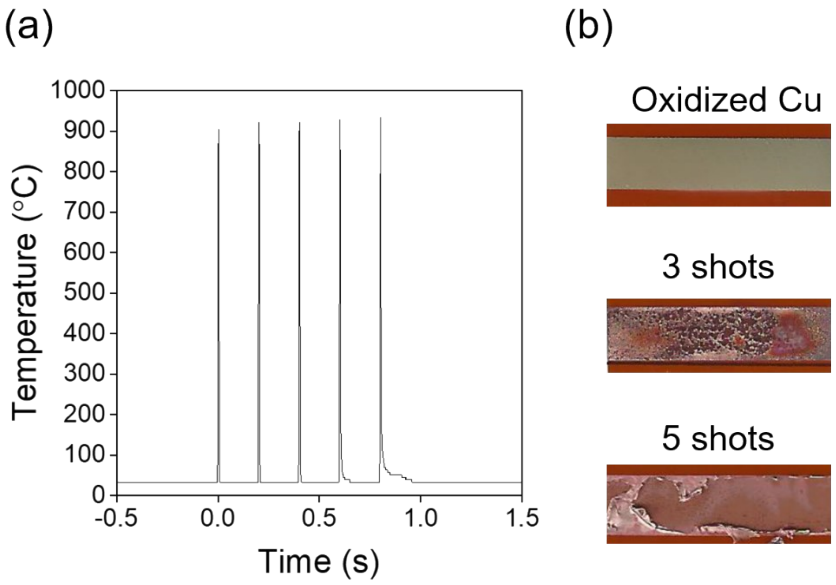


**Fig S6**. (a) Measured temperature variation of oxidized Cu sub-μP patterns during multi-pulse IPL irradiation and (b) photographs of sintered Cu sub-μP patterns for each condition.

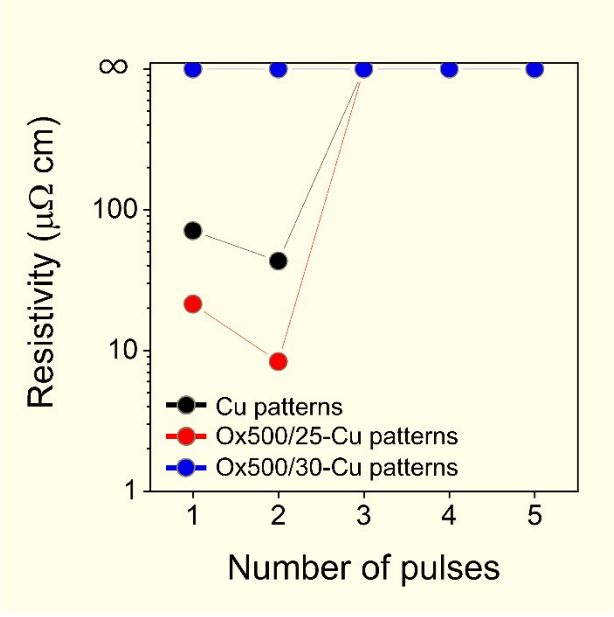


**Fig S7**. Measured electrical resistivities of bare Cu, Ox500/25, and Ox500/30-Cu sub-μP electrodes during multiple IPL irradiation for pulse repetition rate of 1.0 Hz with 5 shots.

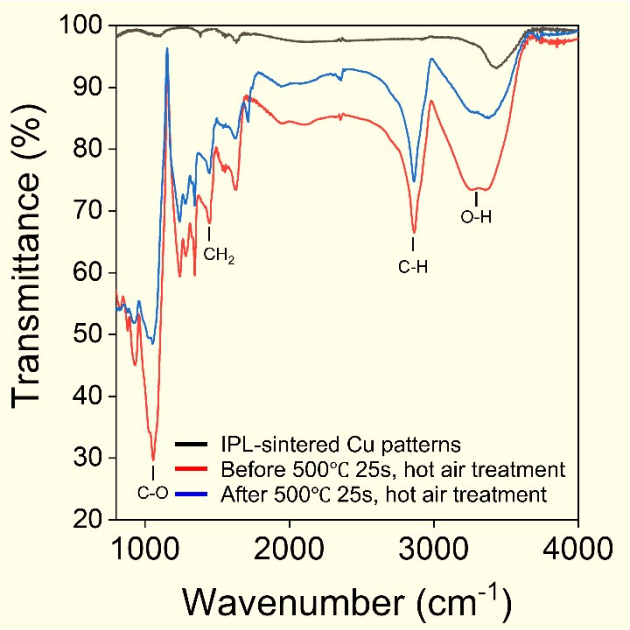


**Fig S8**. FTIR spectra of printed Cu patterns before and after 500 ℃-25 s hot air treatments.

According to the FT-IR spectra, the broad band at 3294 $cm^{-1}$ and 2938 $cm^{-1}$ related to the stretching vibration of the O-H group and C-H in ethylene glycol. In addition, EG-vibrational bands at 1452 $cm^{-1}$ to the $CH_2$ bending, and 1069 $cm^{-1}$ to functional groups, namely C-O stretching.

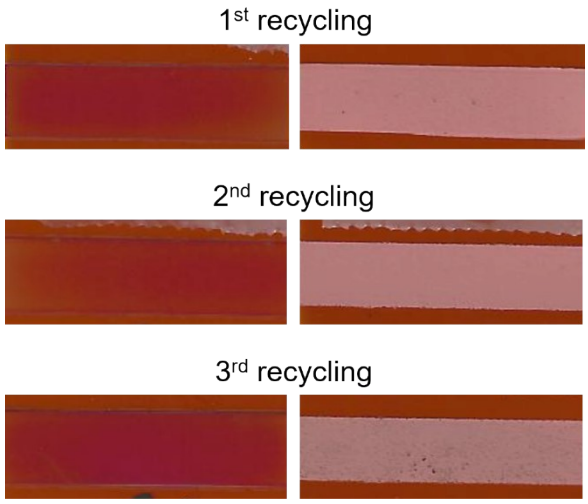


**Fig S9**. Photographs of Cu sub-μP patterns during recycling test.

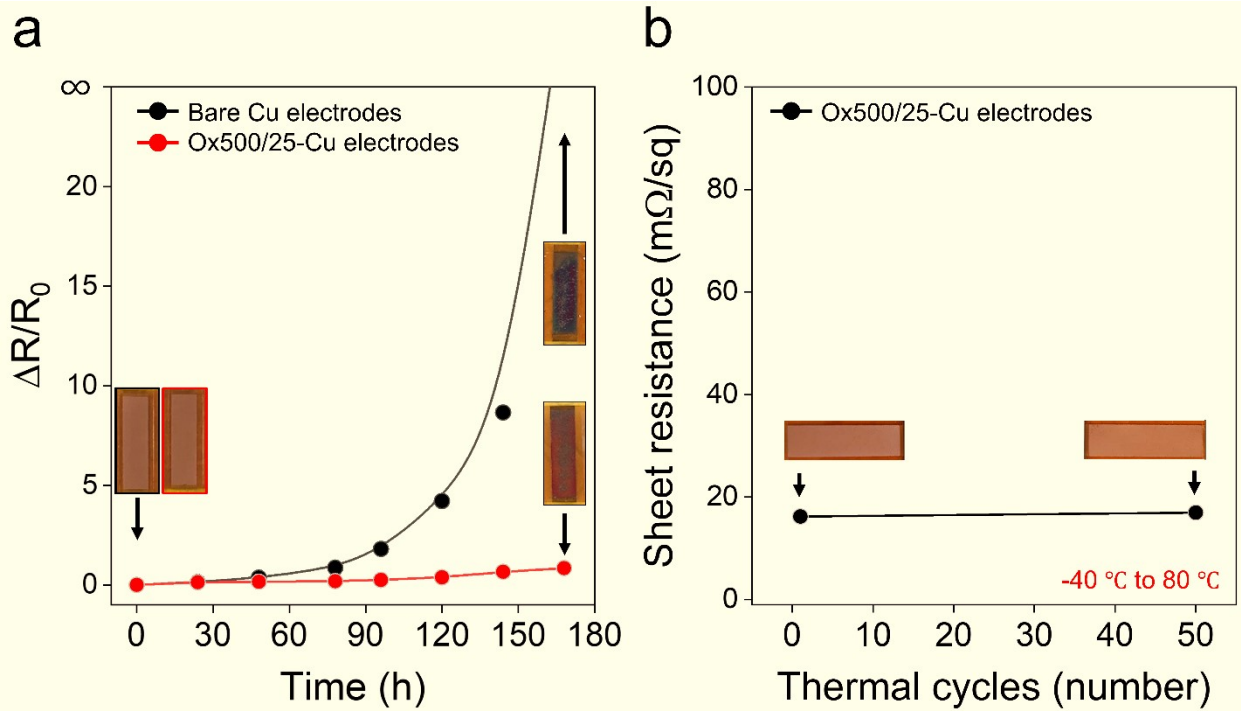


**Fig S10**. Variation of the normalized resistance with time for the bare Cu patterns and Ox500/25-Cu μP electrodes during environmental stability tests under (a) 85℃/RH85% and (b) thermal shock (-40 to 80 ℃, 50 cycles)

To investigate the oxidation resistance of sintered Cu μP electrodes, we have conducted a temperature and humidity test (85 ℃/RH85 %) of the bare Cu and Ox500/25-Cu μP sintered electrodes for 168 hours. After the test for 168 hours, the normalized resistance varied, with values of 9.14 and 0.84 for the bare-Cu and Ox500/25-Cu μP sintered electrodes, respectively. Also, in the thermal shock test (-40 ℃ to 80 ℃), the electrical performance of the Ox500/25-Cu μP sintered electrodes did not deteriorate even after 50 cycles (50 hours). These results showed that Ox500/25-Cu μP sintered electrodes had higher oxidation resistance and thermal shock resistance due to their high densification levels and uniformly sintered morphologies than the bare Cu sintered electrodes.

| Strategy | Energy density ($J\ cm^{-2}$) | Number of pulses | Resistivity (μΩ cm) | Substrate | Reference |
|---|---|---|---|---|---|
| Cu microparticles | 4 | 5 | 9.54 | PI | 1 |
| Cu microparticles | 7 | 1 | 16 | PI | 2 |
| Cu microparticles/ Cu nanoparticles | 12.5 | 1 | 72.8 | PI | 3 |
| Bimodal Cu nanoparticles | 6 | 5 | 5.68 | PI | 4 |
| CuO nanoparticles | 11.7 | 1 | 9 | Silica coated PET | 5 |
| Cu nanoparticles/ CuO nanoparticles | 3.08 | 1 | 70 | PI | 6 |
| $Cu/Cu_2O$ precursor | 17.23 | 10 | 94 | PET | 7 |
| Cu nanoparticles/Cu MOD | 2.7 and 2.9 | 1 | 18.2 | PI | 8 |
| Cu precursor/nanoparticles | 5.17 | 1 | 12.2 | PI | 9 |
| Cu nitrate hydroxide | 12.8 | 40 | 125 | Glass | 10 |
| This work | 7 | 2 | 8.34 | PI | |

**Table S1.** Comparison of previously reported works on IPL sintering of Cu based-patterns with the present study in terms of the Cu filler type, IPL sintering conditions, and electrical performance.

## References


1 J.-W. Lee, J. H. Kwak, J. Kim, S. Jeong, J. H. Park, S. Y. Jeong, S. H. Seo, J. T. Han, G.-W. Lee, K.-J. Baeg, I. H.-S. Yang, H. J. Jeong, *Adv. Mater. Interfaces*, 2021, **8**, 2100769.

2 J.-W. Lee, J. Kim, J. H. Kwak, J. H. Kim, S. Jeong, J. T. Han, G.-W. Lee, K.-J. Baeg, K.-S. Hong, I. H.-S. Yang, H. J. Jeong, *J. Mater. Chem. C*, 2022, **10**, 17336

3 S.-J. Joo, H.-J. Hwang, H.-S. Kim, *Nanotechnology*, 2014, **25**, 265601.

4 M.-H. Yu, S.-J. Joo, H.-S. Kim, *Nanotechnology*, 2017, **28**, 205205.

5 C. Paquet, R. James, A. J. Kell, O. Mozenson, J. Ferrigno, S. Lafrenière, P. R. L. Malenfant, *Organic Electronics*, 2014, **15**, 1836.

6 W.-Y. Chung, Y.-C. Lai, T. Yonezawa, Y.-C. Liao, *Nanomaterials*, 2019, **9**, 1071.

7 R. Dharmadasa, M. Jha, D. A. Amos, T. Druffel, *ACS Appl. Mater. Interfaces*, 2013, **5**, 13227.

8 B. Deore, C. Paquet, A. J. Kell, T. Lacelle, X. Liu, O. Mozenson, G. Lopinski, G. Brzezina, C. Guo, S. Lafrenière, P. R. L. Malenfant, *ACS Appl. Mater. Interfaces*, 2019, **11**, 38880.

9 Y.-R. Jang, R. Jeong, H.-S. Kim, S. S. Park, *Scientific Reports*, 2021, **11**, 14551.

10 G. L. Draper, R. Dharmadasa, M. E. Staats, B. W. Lavery, T. Druffel, *ACS Appl. Mater. Interfaces*, 2015, **7**, 16478.